UDK 669.14.018.62:621.791
Original scientific article/Izvirni znanstveni članek

ISSN 1580-2949
Mater. Tehnol.

EFFECT OF WELDING PARAMETERS ON MECHANICAL AND MICROSTRUCTURAL PROPERTIES OF COLD METAL TRANSFER-WELDED THIN SHEET AISI 301LN STAINLESS STEEL

VPLIV PARAMETROV VARJENJA NA MEHANSKE IN MIKROSTRUKTURNE LASTNOSTI MEDSEBOJNO ZVARJENIH TANKIH PLOČEVIN IZ NERJAVNEGA JEKLA AISI 301 LN S POSTOPKOM PRENOSA KAPLJIC TALINE NA HLADNO KOVINO

A. Ramakrishnan*, Rameshkumar Thirupathi

Department of Mechanical Engineering, Bannari Amman Institute of Technology, Erode 638401, India

Prejem rokopisa – received: 2024-10-21; sprejem za objavo – accepted for publication: 2025-02-04

doi:10.17222/mit.2024.1332

Joining thin plates is a significant challenge in manufacturing, demanding precise control to produce high-strength, spatter-free welds. Cold metal transfer (CMT) welding, known for its minimal heat input, is a promising solution for this challenge. This study looks into the welding of AISI 301LN stainless steel thin sheets using the CMT technique, specifically the influence of important parameters such as welding current (I), welding speed (S), and contact-tip-to-workpiece distance (CTWD). Fractographic investigation using FESEM revealed characteristic dimpled and crack-free tensile fracture surfaces, indicating high mechanical integrity. Among the parameters, welding speed (S) had a highly influential impact on tensile strength, followed by welding current (I) and contact-tip-to-workpiece distance (CTWD). Ideal welding conditions include a current of 100 A, a speed of 4 mm/sec, and a CTWD of 7 mm, producing welds with exceptional mechanical characteristics, complete penetration and a significant, 24.10 % increase in tensile strength. A drop in the microhardness of the weld zone is observed due to the formation of dendrites.

Keywords: cold metal transfer welding, 301LN, tensile strength, hardness, contact-tip-to-workpiece distance

Medsebojno spajanje tankih pločevin je posebno zahtevno in predstavlja pravi izziv za proizvodnjo zaradi velikih zahtev glede toleranc, visoke trdnosti spojev, brez navarkov in obrizgov. Postopek varjenja s prenosom kapljic taline z elektrode na hladno kovino (CMT; angl.: Cold Metal Transfer welding) je postopek z minimalnim vnosom toplotne energije v material, ki ga spajamoin zato predstavlja obetajoč postopek za rešitev tega problema.V tem članku avtorji predstavljajo študijo varjenja (spajanja) tankih pločevin iz nerjavnega jekla vrste AISI 301LN s tehniko CMT varjenja. Pri tem so avtorji analizirali vpliv posameznih procesnih parametrov varjenja kot so: električni tok varjenja (I), hitrost varjenja (S) in razdalja med vrhom konice elektrode in varjencem(CTWD; angl.:contact-to-work distance). Fraktografske preiskave prelomov s pomočjo vrstičnega elektronskega mikroskopa na emisijo polja (FESEM; field emission scanning electron microscope) so odkrile karakteristično duktilni jamičasti prelom brez razpokna nateznih preizkušancih. To je potrdilo, da imajo zvari visoko mehansko integriteto. Med procesnimi parametri je imela hitrost varjenja S največji vplivna natezno trdnost, sledila sta električni tok varjenjaI in razdalja med vrhom konice elektrode in varjencem CTWD. Idealne pogoje varjenja so avtorji dosegli pri I je 100 A, hitrosti S je 4 mm/s in CTWD je 7 mm. Pri teh pogojih varjenja so dosegli izjemne mehanske lastnosti s popolno penetracijo taline in pomembnim 24,1 povečanjem natezne trdnosti v primerjavi s preizkušancem številka 4. Meritve mikrotrdote zvarov so pokazale njen padec v zvarni coni zaradi tvorbe dendritov med strjevanjem.

Keywords: postopek varjenja s prenosom kapljic taline z elektrode na hladno kovino, nerjavno jeklo vrste AISI 301LN, natezna trdnost, trdota, razdalja med vrhom konice in varjencem

1 INTRODUCTION

Material science research and development has seen tremendous growth due to the need for high-performance materials in a range of industrial applications. 301LN is a nitrogen-enhanced austenitic stainless steel with a low nickel content. Nitrogen in stainless steel improves the metal's corrosion resistance as compared to the applicable grades 301 and 301L. A low nickel concentration makes steel more cost effective than other nickel-containing steels. Low nickel levels reduce the metal's strength, which is compensated for by adding nitrogen. Low carbon concentration reduces carbide precipitation during the welding process, improving corrosion resistance characteristics. Adding to its advantages, 301LN exhibits high weldability and flexibility, making it perfect for creating complicated forms and components using various forming processes such as stamping, bending, drawing, and welding. The material is also recyclable and durable, which lowers maintenance costs and supports material sustainability. The material is used in aerospace, vehicle, industrial equipment manufacture,

*Corresponding author's e-mail:
ramkrishmechstar@gmail.com (A. Ramakrishnan)

Table 1: Chemical composition (%) of 301LN and 308L

Element	Fe	Cr	Ni	Mn	Si	N	P	C	S
301LN	Rem.	16	6	2	1	0.20	0.045	0.03	0.03
308L	Rem.	19.5	9	2	1.25	-	0.03	0.03	0.03

structural applications, railway coach construction, and other industries. Welding is required for constructing larger components.

Conventional welding processes, such as metal inert gas (MIG) and tungsten inert gas (TIG), often require a large amount of heat during the welding process. Excessive heat can reduce the mechanical strength of the welded material and cause the creation of undesired weld zones, jeopardising the structure's overall integrity. In contrast, the cold metal transfer (CMT) welding is a low heat input approach that provides substantial benefits in terms of retaining the base material's mechanical qualities. CMT welding lowers thermal distortion and the possibility of flaws including grain development, sensitisation, and phase transitions, which are frequent in traditional high-heat welding processes. As a result, CMT welding is exceptionally good at retaining material strength and toughness, making it a top choice for applications requiring mechanical performance.

Recent studies on microstructure evolution via various welding processes have demonstrated significant improvements in mechanical properties. Jayantha Ghosh Roy et al. investigated 304 stainless steel welded using CMT, reporting an optimal UTS of 729 MPa, 117 % elongation, and 282.4 HV, with residual stress and dimpled morphology observed[1]. Jie Zhou et al. found that AISI 430 ferritic steel welded with a 308L filler rod exhibited fractures in the base metal rather than the weld zone, indicating enhanced properties.[2] Pickin et al. highlighted the versatility of CMT's short circuit and spray transfer modes in achieving desired weld compositions.[3] Kumar et al. explored the impact of sensitization and thermal ageing on micro-hardness and corrosion in AISI 304 welded joints.[4] Jarvenpaa et al. studied laser welding of 301LN steel, noting coarse grains and a narrow HAZ, with failures occurring due to microsegregation.[5] Wei Liu et al. examined spot welding of CRHS 301LN sheets, finding that interface folding affected fatigue performance.[6] Seung Hwan Lee et al. optimized WAAM parameters to improve shape quality,[7] while Chen Zhou et al. investigated CMT droplet dynamics influenced by magnetic arc flow.[8] Srikanth et al. showed that cold reductions and reversion annealing at 750 °C of 301LN grade coils enhanced their properties through grain refinement.[9] Additionally, Antti Jarvenpaa et al. demonstrated that reversion treatment could yield stainless steel with superior strength, elongation, and fatigue resistance.[10] Ghanasekaran et al. achieved a yield strength of 833 MPa and tensile strength of 980 MPa in 301 stainless steel joints using laser welding, with high cooling rates leading to fine grain formation in the weld region.[11]

Even though considerable research on the welding of AISI 301 austenitic stainless steel has been carried out, there is a significant void in the literature regarding the use of cold metal transfer (CMT) welding on AISI 301LN. No previous research has comprehensively investigated the effects of CMT welding on the tensile characteristics, microstructure, and overall performance of AISI 301LN joints. This study aims to fill that gap by assessing the application and benefits of CMT welding for AISI 301LN stainless steel, including its capacity to improve weld quality and mechanical qualities. The study examines the impact of CMT welding on the mechanical properties of 301LN stainless steel, demonstrating that low heat input welding may maintain the integrity of high-performance materials. We want to demonstrate the advantages of CMT in preserving superior weld quality and performance by comparing the tensile strength, ductility, and microstructural properties of CMT welds to those created using conventional methods.

2 EXPERIMENTAL PART

A whole sheet of (2 × 1500 × 2000) mm 301LN material was purchased. To prepare welding samples, the sheet was first cut into smaller portions with a manual shear cutter. The required sample dimensions of (150 × 100 × 2) mm were then attained using a hydraulic press, as shown in **Figure 1a**. The hydraulic press was used for cutting to prevent changes in mechanical and microstructural qualities caused by heat-based cutting processes. The chemical composition of the base metal 301LN and filler rod 308L is shown in **Table 1**. In the first step of the investigation, we performed a thorough examination to evaluate the microstructural and mechanical characteristics of 301LN stainless steel as shown in Figure 1b. Tensile test specimens were precisely cut utilising wire-cut electrical discharge machining (EDM) per ASTM standards, as shown in **Figure 1c**.[1]

These specimens were then tensile tested using a cutting-edge computerised tensile testing system, resulting in an ultimate tensile strength of 830 MPa. Concurrently, we conducted a comprehensive hardness study of the base metal with an HDNS-Kelly Instruments micro-Vickers hardness tester and a 0.5 kg load, yielding an average hardness of 277 HV, highlighting the material resilience and resistance to localised deformation. Furthermore, the microstructural characteristics of the base metal were thoroughly studied using sophisticated microscopy techniques, resulting in high-resolution photographs that revealed the material internal composition. Scanning electron microscopy (SEM) was used to ad-

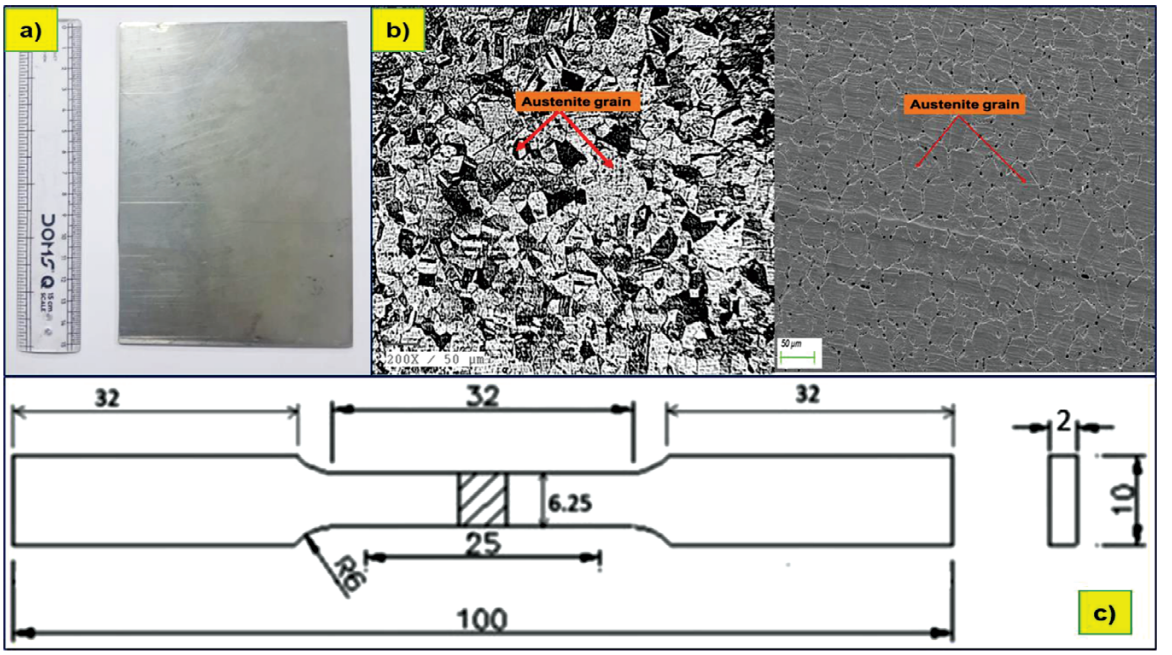

Figure 1: Photographs of a sample: a) microstructure before welding, b) welded sample, c) CAD model of a tensile sample as per ASTM before welding

vance our investigation, providing a precise picture of the surface morphology and deepening our understanding of the microstructural properties of 301LN stainless steel. In this experimental investigation, 99.99 % pure argon was used as the shielding gas. During welding, the shielding gas interacts with the filler metal, leading to microstructural changes that influence the mechanical properties and corrosion resistance of the weld deposits. Cold metal transfer (CMT) welding, an automated MIG process with controlled arc characteristics, was employed using a 1.2 mm diameter 308L filler rod. The CMT welding machine used in this experiment is shown in **Figure 2a** while a simplified schematic diagram is provided in **Figure 2b**.

2.1 Design of experiment

Initial results showed that sufficient strength and full penetration were not achieved in the samples. To address this, the welding speed was fixed at 4 mm/sec, and the contact-tip-to-workpiece distance was adjusted to 7 mm. The current was then increased to further refine the welding process. The Taguchi method was implemented to plan and carry out an experimental design in this investigation. To carry out the design of experiments, a thorough examination of three important parameters and their relative levels was conducted, guided by preliminary trial tests. Following this extensive investigation and literature analysis, welding current (I), welding speed (S), and contact-tip-to-workpiece distance

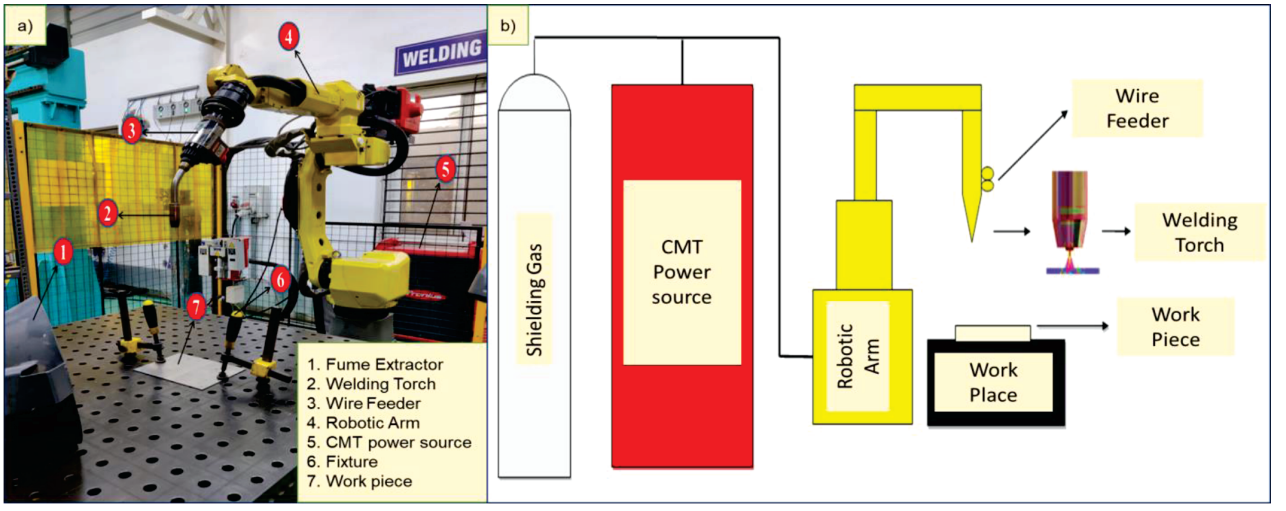

Figure 2: a) CMT welding machine set-up, b) schematic diagram

Table 2: Impact of process parameters on CMT welding of AISI 301LN stainless steel

S. No.	1	2	3	4	5	6	7	8	9
Welding current (I) – A	90	90	90	95	95	95	100	100	100
Welding speed (S) – mm/sec	4	6	8	4	6	8	4	6	8
Contact-tip-to-workpiece distance (CTWD) – mm	3	5	7	5	7	3	7	3	5

(CTWD) were identified as the characteristics impacting the welding process.[1] The welding current (I) was set to three different levels: (90, 95, and 100) A. Concurrently, the welding speed (S) was studied at three different levels: 4, 6, and 8 mm/sec, while the contact-tip-to- workpiece distance (CTWD) was measured at 3-, 5-, and 7-mm intervals. As shown in **Table 2**, this design of experiment framework enabled us to completely evaluate the impact of these welding factors on the welding process, resulting in improved performance.

3 RESULTS AND DISCUSSION

3.1 Welded samples and heat input

The welding was performed effectively, and the weld samples are shown in **Figure 3a**. A splatter-free weld was produced. Visual inspection revealed that the samples had an adequate weld bead shape, but none of them achieved complete penetration. The penetration depth improved as the current (A) value increased. When the welding speed was raised, irregular weld bead patterns appeared. Following these findings, the current was increased to 100 A. Under increased current, the sample obtained a weld bead with full penetration, as shown in **Figure 3b**. In welding, several factors critically influence the heat input, thus they are essential for achieving efficient and effective welds as shown in **Figure 3c**.

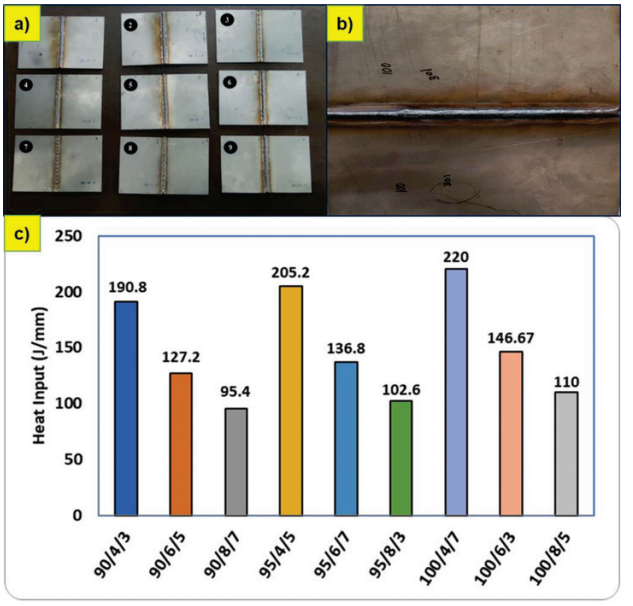

Figure 3: a) Photograph of a sample after welding, b) sample weld with increased current, and c) testing heat input with different samples

Heat input is a critical parameter in welding that influences the microstructure, mechanical properties, and quality of the weld joint. Optimal heat input controls the depth of penetration, weld bead shape, and hydrogen absorption, ensuring a strong and durable weld. Key variables include voltage (V), current (I), welding speed (S), and the efficiency (η) of the welding process. It was observed that as the welding speed increased, the heat input decreased by 33.3 % when comparing Samples 1 and 2, and by 25 % when comparing Samples 2 and 3. Conversely, increasing the current at a constant welding speed results in a higher heat input, with a 7 % rise observed from Samples 1 to 4, and a 6.7 % increase observed from Samples 4 to 7. Achieving full fusion throughout the material's thickness is vital in the welding process, as demonstrated with Sample 7, where a 6.7 % increase in the heat input over Sample 4 led to complete fusion. Thus, higher welding speeds typically reduce heat input, while increasing current tends to raise it.

$$\text{Heat Input } (Q) = \eta \frac{VXI}{S}$$

3.2 Macrostructure of the weld

Optical transverse macro cross-sections of CMT-welded samples with similar thicknesses under varying heat input conditions clearly illustrate the significant impact of thermal input on weld bead geometry, particularly penetration depth as shown in **Figures 4a** to **4i**. The macrostructure of a weld joint, an important focus of this research, provides a macroscopic overview of the weld's overall structure and morphology. The study meticulously examined and characterized the weld joint's macrostructure to gain a comprehensive understanding of key features such as weld bead geometry, fusion zone dimensions, heat-affected zone (HAZ), and any observable defects or irregularities. Weld bead profiles for various parameter combinations are shown below, highlighting that single-pass welds often exhibit a lack of penetration. Notably, maximum weld penetration was observed in samples with lower welding speeds. Sample 7, featuring a current of 100 A, welding speed of 4 mm/sec and CTWD of 7 mm achieved full penetration as depicted in **Figure 4g**.

This finding underscores the critical influence of welding speed on penetration depth, with slower speeds leading to improved weld penetration, particularly in the configuration represented by Sample 7, which demonstrated superior penetration compared to the other parameter combinations. As thermal input increases, pene-

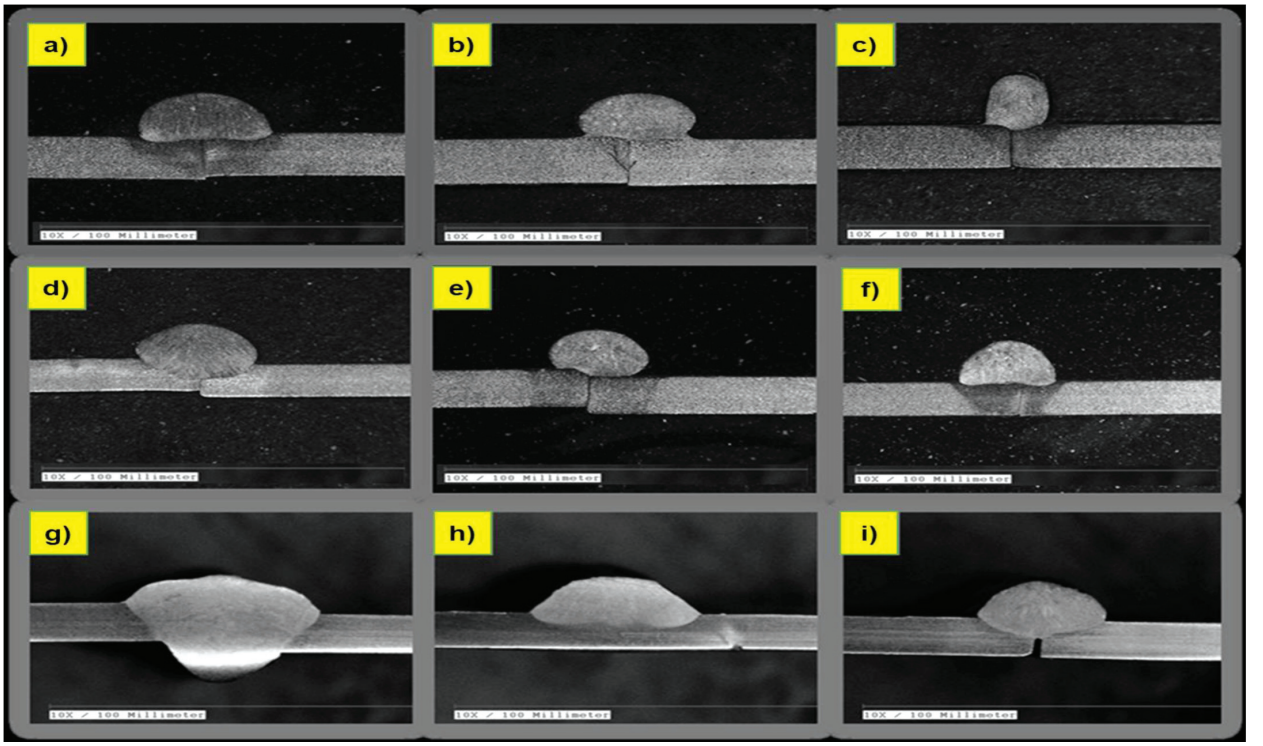

Figure 4: Macrostructure images of CMT-welded samples

tration depth increases due to the lower cooling rate associated with increasing heat inputs. At lower current and higher speed levels, penetration depth is reduced. However, increasing the current while retaining a lower speed increases the penetration depth. The combination of a lower travel speed and a higher welding current is optimal for producing high-quality welds with full penetration.

3.3 Tensile results for the weld

The strength of welded samples varies greatly due to factors such as partial fusion and insufficient penetration during welding, resulting in weaker connections between the weld metal and base metal. This is reflected in lower tensile strength and reduced ductility, as evidenced by the decrease in % elongation, shown in **Figure 5b**. Samples with insufficient penetration shatter brittlely due to the development of brittle intermetallic compounds in the weld zone, as confirmed by energy-dispersive X-ray spectroscopy (EDX), shown in **Figure 9**. The microstructural changes in the weld bead, which are predominantly caused by heat input during welding, influence the balance of austenite and ferrite in the joint. Tensile-tested fracture surfaces exhibit a dimpled shape without cracks, indicating ductile failure with negligible carbide precipitation.[11–14] The weld strength of Sample 4 was 617 MPa, which exceeded the filler rod strength of 530 MPa, providing important insights into the welding process and its impact on material behaviour and structural integrity. In contrast, Sample 7, which showed full penetration, had a greater tensile strength of 813 MPa and a 10 % elongation, indicating a ductile fracture process. This resulted in a significant, 24.10 % improvement in the tensile strength over Sample 4, as shown in **Figure 5a**.

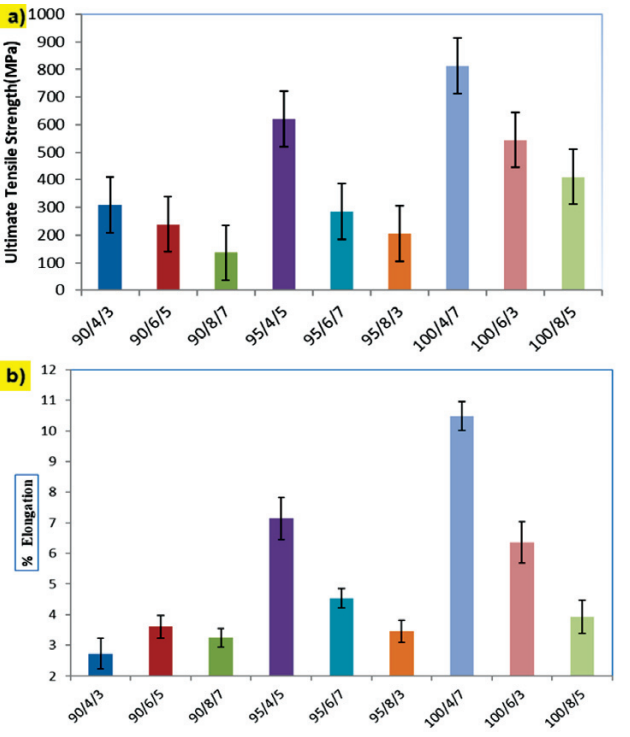

Figure 5: a) Ultimate tensile strength and b) elongation (%)

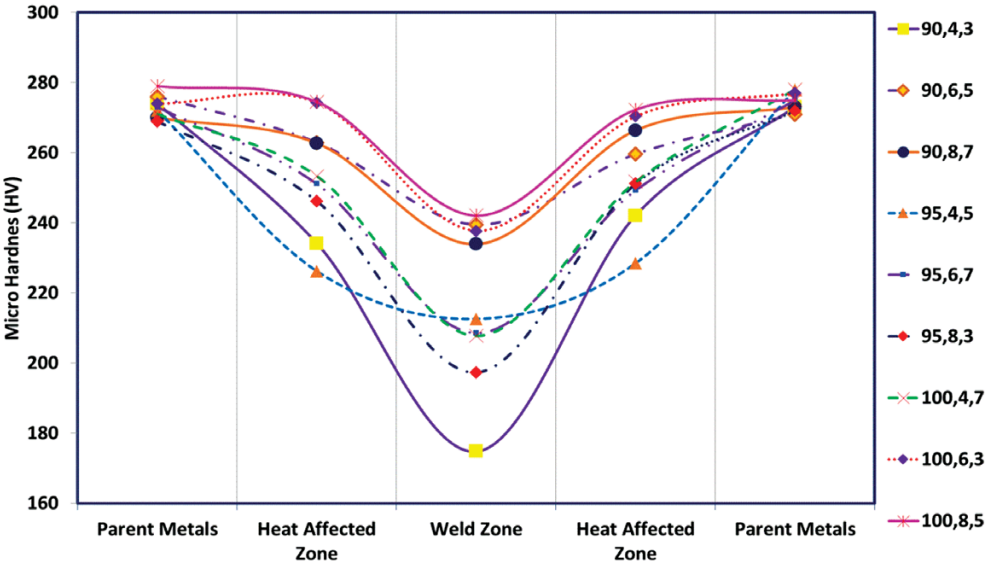

Figure 6: Microhardness of the welded samples

3.4 Microhardness of the weld

Vickers microhardness testing was performed on different regions like the base metal, heat affected zone and weld zone to determine the material hardness which is depicted in **Figure 6**. Samples were taken from the weld area, and square-shaped indentations were made with a Vickers microhardness tester under controlled stresses. Vickers hardness numbers (HV) were calculated using the measurements of these indentations. Multiple indentations were made to capture changes in the hardness throughout the material. The investigation focused on the hardness distribution within the weld joint and heat-affected zone (HAZ), which provided useful insights into the welding process's impacts. Our findings included information about HV levels, testing settings, and observed trends.

The weld zone and HAZ exhibited significantly lower hardness values than the base metal, with the average hardness percentage reduction ranging from 8 % to 25 %. The observed dendritic development in the weld region was identified as a contributor to the decrease in microhardness.[1]

3.5 Microstructure and SEM images of the weld

Microscopic and SEM images of the 301LN welded samples are depicted in **Figures 7a** to **7d** and **8a** to **8d**. They show that there were no thermal cracks or distortions. The optical microscope (OM) image of the base metal shows the presence of austenite and ferrite. In the heat-affected zone (HAZ), grain size refinement is visible when compared to the base metal. **Figure 7c** provides a clear picture of a fusion boundary. Near the top and middle weld boundaries, the microstructure displays ferrite in many forms, including skeleton, vermicular, and lathy structures, which solidified largely as δ-ferrite in the FA mode.[5] In the HAZ, ferrite branches parallel to the rolling direction extend into the weld bead, forming

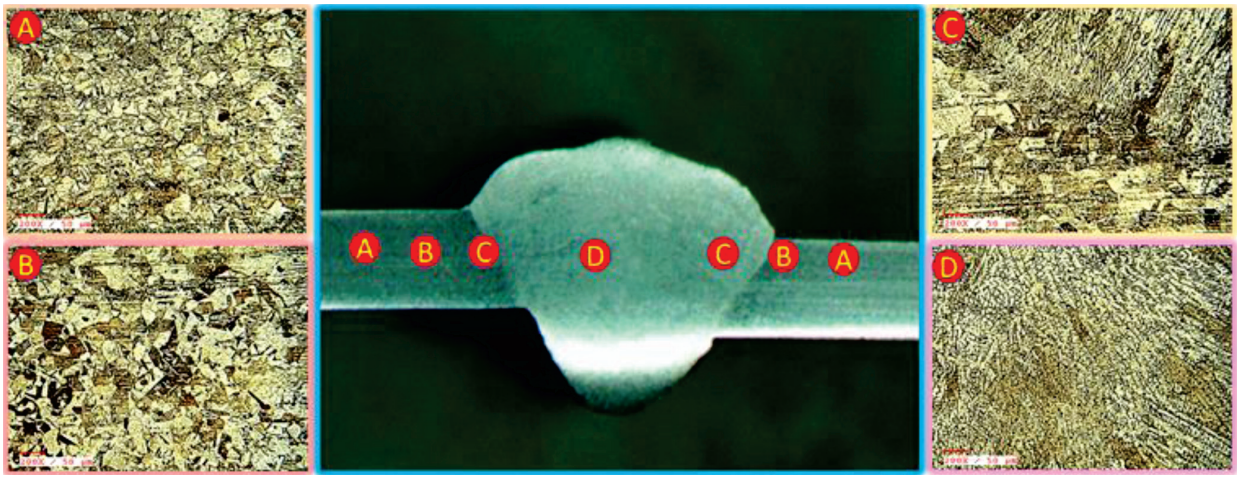

Figure 7: OM images: A) base metal, B) heat affected zone, C) weld interface, D) weld zone

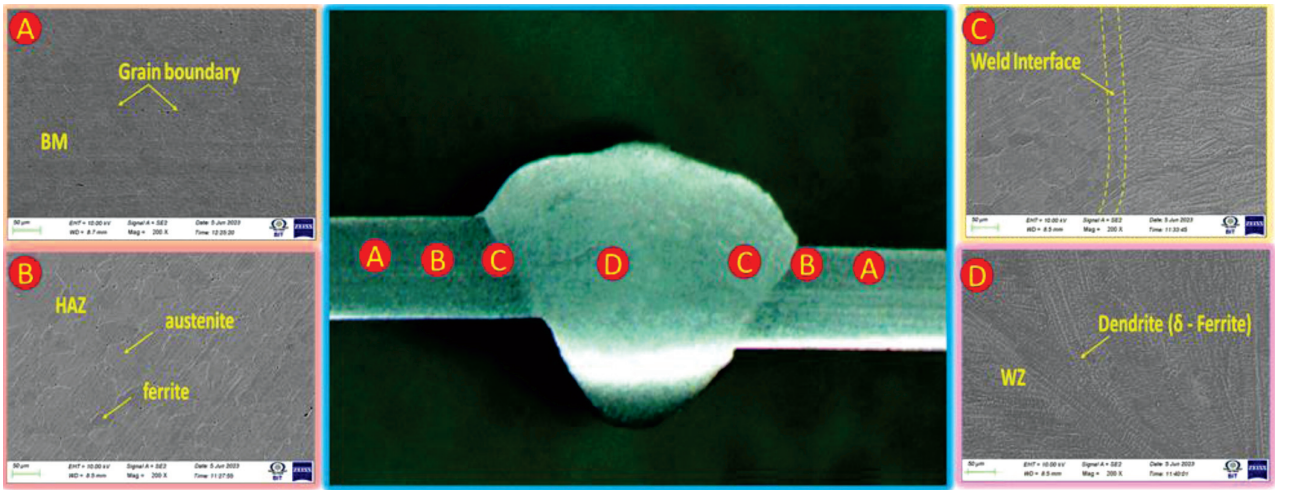

Figure 8: SEM images: A) base metal, B) heat affected zone, C) weld interface, D) weld zone

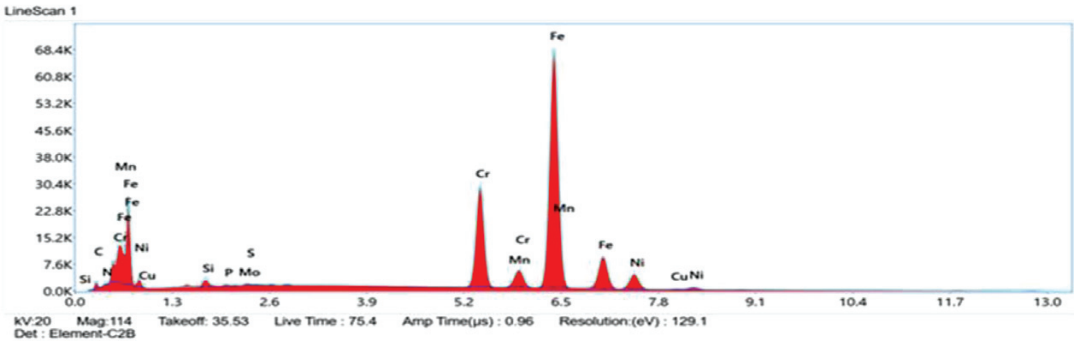

Figure 9: Line scan EDX spectrum of Sample 7

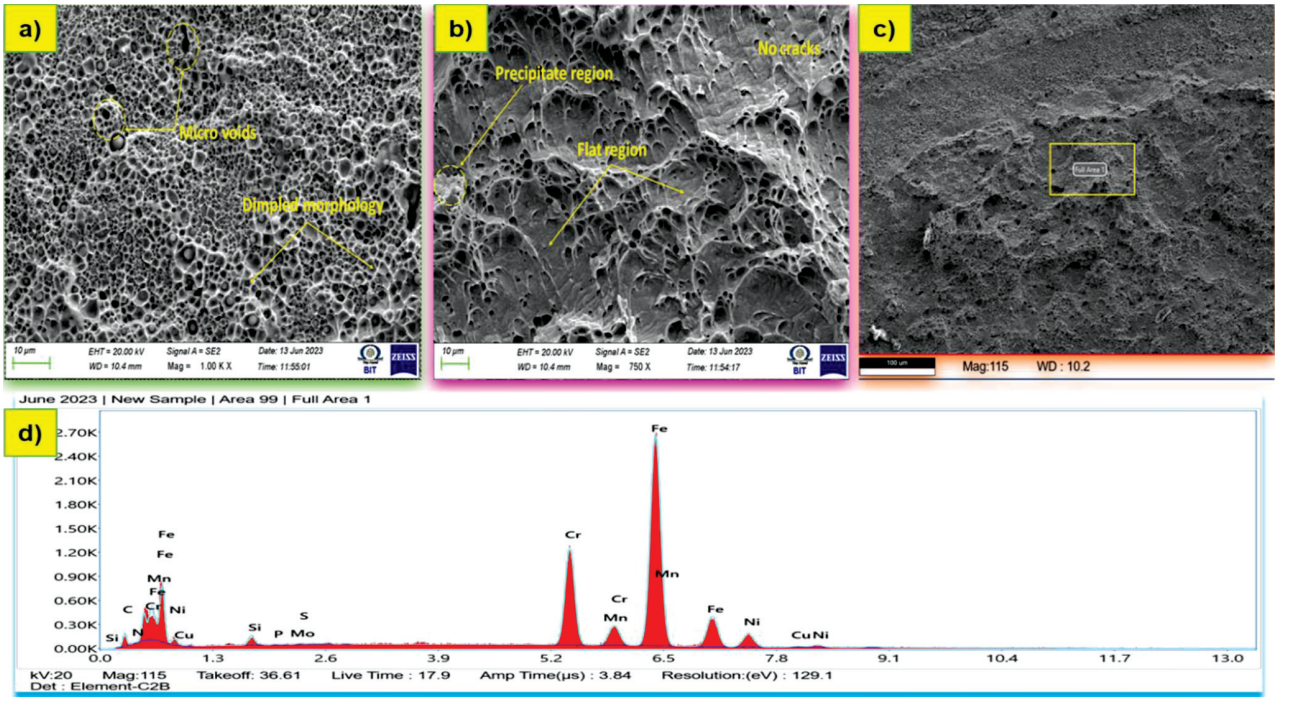

Figure 10: SEM image of the fractured area of the tensile sample with EDX spectrum

secondary arms that serve as nucleation sites for ferrite solidification. Austenite occurs through peritectic interactions between adjacent ferrite dendrites, resulting in a complicated change from δ-ferrite into austenite.

Larger ferrite dendrites are seen in the centre of the upper weld. A mixture of lathy, vermicular, and skeleton ferrites may be seen in the middle weld region, along with some sizable austenite areas, where solidification switches from the FA mode to the A and AF modes. SEM photos demonstrate that larger lathy ferrites occur near the weld centre due to slower cooling rates. During peritectic solidification, δ-ferrite transforms into austenite, which produces these ferrites. Dendritic austenite solidified in the AF mode predominates at the weld root, with some interdendritic eutectic ferrites present.[24] Ferrite crystallises in the FA mode and is manifested as short laths and continuous networks close to the fusion line. The line scan for the weld sample is shown in **Figure 9**. Fewer ferrites are found inside the dendritic core as the ferrite networks become discontinuous close to the weld centre. The material's resistance to thermal cracking is increased due to the ferrite network, which is essential for pinning grain boundaries.

3.6 Fractography of the fractured weld

The fractured area of the tensile sample is being studied. The welded parts show ductile fracture due to the creation of massive micro and sub-micro voids generated by high-stress concentration, as shown in **Figure 10**.

The fracture surface has a dimpled pattern with no apparent fissures, indicating a ductile fracture, due to which the material stretched extensively before breaking. Dimples of varying sizes are visible, with certain locations exhibiting greater voids due to high-stress concentration during the tensile testing. The presence of these dimples indicates that the material exhibits high ductility, which means it may extend easily, increasing the strength of the weld joint. The chemical strengthens the weld joint and causes increased elongation. Some fracture edges show that certain areas experienced brittle fracture.[28]

4 CONCLUSIONS

Our welding approach effectively yielded splatter-free welds with excellent bead geometry, despite the initial failures to achieve full penetration in the samples. It was found that increasing the current value enhanced penetration depth, whereas increasing the welding speed led to uneven bead patterns.

Full penetration of the weld bead was obtained by increasing the current to 100 A, as evidenced by the final test sample. Sample 7, which achieved complete penetration, exhibited better tensile qualities, with a tensile strength of 813 MPa and 10 % elongation. This shows a significant, 24.10 % improvement in the tensile strength over Sample 4.

Vickers microhardness testing revealed a significant reduction in the hardness within the weld and heat-affected zone, with decreases ranging from 8 to 25 % compared to the base metal. This reduction is attributed to the dendrite formation during the welding process.

The microstructure of the 301LN welded sample showed no signs of thermal cracks or distortion. Its images highlighted a refined grain structure in the heat-affected zone and complex transformations from δ-ferrite to austenite, contributing to the material's resistance to thermal cracking.

A dimpled fracture surface implies a primarily ductile fracture, with significant material elongation before failure. However, the presence of some brittle fracture zones indicates that the material's stress response is variable.

5 REFERENCES

[1] Jayanta Ghosh Roy, N. Yuvaraj, Vipin, Effect of Welding Parameters on Mechanical Properties of Cold Metal Transfer Welded Thin AISI 304 Stainless-Steel Sheets, Transactions of the Indian Institute of Metals, 74 (**2021**), 2397–2408, doi:10.1007/s12666-021-02326-2

[2] Jie Zhou, Junqi Shen, Shengsun Hu, Guancheng Zhao, Qian Wang, Microstructure and mechanical properties of AISI 430 ferritic stainless steel joints fabricated by cold metal transfer welding, Mater. Res. Express, 6 (**2019**) 11, 116536, doi:10.1088/2053-1591/ab4770/meta

[3] C. G. Pickin, S. W. Williams, M. Lunt, Characterisation of the cold metal transfer (CMT) process and its application for low dilution cladding, Journal of Materials Processing Technology, 211 (**2011**) 3, 496–502, doi:10.1016/j.jmatprotec.2010.11.005

[4] M. Kumar, A. Babbar, A. Sharma, A. S. Shahi, Effect of post weld thermal aging (PWTA) sensitization on micro-hardness and corrosion behavior of AISI 304 weld joints, J. Phys.: Conf. Ser., 1240 (**2019**) 01, 2078, doi:10.1088/1742-6596/1240/1/012078/meta

[5] A. Järvenpää, M. Jaskari, M. Keskitalo, K. Mäntyjärvi, P. Karjalainen, Microstructure and mechanical properties of laser-welded high-strength AISI 301LN steel in reversion-treated and temper-rolled conditions, Procedia Manufacturing, 36 (**2019**), 216–223, doi:10.1016/j.promfg.2019.08.028

[6] Wei Liu, Runjiao Wang, Junlei Han, Xiangyang Xu, Qiang Li, Microstructure and mechanical performance of resistance spot-welded cold-rolled high strength austenitic stainless steel, Journal of Materials Processing Technology, 210 (**2010**) 14, 1956–1961, doi:10.1016/j.jmatprotec.2010.07.008

[7] Seung Hwan Lee, Optimization of cold metal transfer-based wire arc additive manufacturing processes using gaussian process regression, Metals, 10 (**2020**) 4, 461, doi:10.3390/met10040461

[8] Jie Zhou, Junqi Shen, Shengsun Hu, Guancheng Zhao, Qian Wang, Microstructure and mechanical properties of AISI 430 ferritic stainless steel joints fabricated by cold metal transfer welding, Materials Research Express, 6 (**2019**) 11, 116536, doi:10.1088/2053-1591/ab4770/meta

[9] S. Srikanth, P. Saravanan, Vinod Kumar, D. Saravanan, L. Sivakumar, S. Sisodia, K. Ravi, B. K. Jha, Property enhancement in metastable 301LN austenitic stainless steel through strain-induced martensitic transformation and its reversion (SIMTR) for metro coach manufacture, Int. J. Metall. Eng., 2 (**2013**) 2, 203–213, doi:10.5923/j.ijmee.20130202.12

[10] Antti Järvenpää, Matias Jaskari, Anna Kisko, Pentti Karjalainen, Processing and properties of reversion-treated austenitic stainless steels, Metals, 10 (**2020**) 2, 281, doi:10.3390/met10020281

[11] S.Gnanasekaran, S. Senthil Kumar, Narasimharaj Venugopal, Makarand Upadhyaya, T. C. Manjunath, Samson Jerold Samuel Chelladurai, G. Padmanaban, Effect of laser power on microstructure and tensile properties of pulsed Nd: YAG laser beam welded AISI 301 austenitic stainless steel joints, Materials Today: Proceedings, 37 (**2021**) 2, 934–939, doi:10.1016/j.matpr.2020.06.145

[12] Chen Zhou, Hongliang Wang, Thomas A. Perry, James G. Schroth, On the analysis of metal droplets during cold metal transfer, Procedia Manufacturing, 10 (**2017**), 694–707, doi:10.1016/j.promfg.2017.07.024

[13] T. Srikanth, S. Surendran, G. Balaganesan, G. L. Manjunath, Response of CMT welded aluminum AA5086-H111 to AA6061-T6 plate with AA4043 filler for ballistic, Procedia Engineering, 194 (**2017**), 522–528, doi:10.1016/j.proeng.2017.08.180

[14] Jun-xia Huang, Xiao-ning Ye, Zhou Xu, Effect of cold rolling on microstructure and mechanical properties of AISI 301LN metastable austenitic stainless steels, Journal of Iron and Steel Research International, 19 (**2012**) 10, 59–63, doi:10.1016/S1006-706X(12)60153-8

[15] Xiqing Li, Wei Liu, Xiangzhong Guo, Zhiguo Zhang, Zhikun Song, Microstructure Evolution of Laser Welded 301LN and AISI 304 Austenitic Stainless Steel, Metallurgical and Materials Transactions A, 54 (**2023**) 4, 1186–1198, doi:10.1007/s11661-023-06973-6

[16] Subodh Kumar, A. S. Shahi, Studies on metallurgical and impact toughness behavior of variably sensitized weld metal and heat affected zone of AISI 304L welds, Materials & Design, 89 (**2016**), 399–412, doi:10.1016/j.matdes.2015.09.145

[17] Payam Farhadipour, Shayan Dehghan, Noureddine Barka, Asim Iltaf, Pedram Farhadipour, A study on effect of laser overlay welding parameters of stainless steel 301 LN: tensile test, microstructure analysis and microhardness evaluation, Welding International, 38 (**2024**) 6, 409–421, doi:10.1080/09507116.2024.2342342

[18] A. Evangeline, P. Sathiya, Cold metal arc transfer (CMT) metal deposition of Inconel 625 superalloy on 316 L austenitic stainless steel: microstructural evaluation, corrosion and wear resistance properties, Materials Research Express, 6 (2019) 6, 066516, doi:10.1088/2053-1591/ab0a10/meta

[19] Antti Järvenpää, Matias Jaskari, L. Pentti Karjalainen, Properties of Induction Reversion-Refined Microstructures of AISI 301LN under Monotonic, Cyclic and Rolling Deformation, Materials Science Forum, 941 (**2019**), 601–607, doi:10.4028/www.scientific.net/MSF.941.601

[20] Ahmed Elrefaey, Nigel G. Ross, Microstructure and mechanical properties of cold metal transfer welding similar and dissimilar aluminum alloys, Acta Metallurgica Sinica, 28 (**2015**), 715–724, doi:10.1007/s40195-015-0252-6

[21] Xiaohui Chen, Jia Li, Xu Cheng, Bei He, Huaming Wang, Zheng Huang, Microstructure and mechanical properties of the austenitic stainless steel 316L fabricated by gas metal arc additive manufacturing, Materials Science and Engineering: A, 703 (**2017**), 567–577, doi:10.1016/j.msea.2017.05.024

[22] B. Ravi Kumar, Sailaja Sharma, B. Mahato, Formation of ultrafine grained microstructure in the austenitic stainless steel and its impact on tensile properties, Materials Science and Engineering: A, 528 (2011) 6, 2209–2216, doi:10.1016/j.msea.2010.11.034

[23] S. Selvi, A. Vishvaksenan, E. Rajasekar, Cold metal transfer (CMT) technology – An overview, Defence Technology, 14 (**2018**) 1, 28–44, doi:10.1016/j.dt.2017.08.002

[24] Peng Wang, Shengsun Hu, Junqi Shen, Ying Liang, Jie Pang, Effects of electrode positive/negative ratio on microstructure and mechanical properties of Mg/Al dissimilar variable polarity cold metal transfer welded joints, Materials Science and Engineering: A, 652 (**2016**), 127–135, doi:10.1016/j.msea.2015.11.080

[25] Jie Pang, Shengsun Hu, Junqi Shen, Peng Wang, Ying Liang, Arc characteristics and metal transfer behavior of CMT + P welding process, Journal of Materials Processing Technology, 238 (**2016**), 212–217, doi:10.1016/j.jmatprotec.2016.07.033

[26] Jicai Feng, Hongtao Zhang, Peng He, The CMT short-circuiting metal transfer process and its use in thin aluminium sheets welding, Materials & Design, 30 (**2009**) 5, 1850–1852, doi:10.1016/j.matdes.2008.07.015

[27] C. G. Pickin, S. W. Williams, M. Lunt, Characterisation of the cold metal transfer (CMT) process and its application for low dilution cladding, Journal of Materials Processing Technology, 211 (**2011**) 3, 496–502, doi:10.1016/j.jmatprotec.2010.11.005

[28] S. Ningshen, U. Kamachi Mudali, Pitting and intergranular corrosion resistance of AISI type 301LN stainless steels, Journal of Materials Engineering and Performance, 19 (**2010**), 274–281, doi:10.1007/s11665-009-9441-7